

# Spectrophotometric and Calorimetric Titration Studies on Molecular Recognition of Camphor and Borneol by Nucleobase-Modified $\beta$ -Cyclodextrins

Yu Liu,\* Qian Zhang, and Yong Chen

Department of Chemistry, State Key Laboratory of Elemento-Organic Chemistry, Nankai University, Tianjin 300071, P. R. China

Received: April 16, 2007; In Final Form: August 1, 2007

A series of modified  $\beta$ -cyclodextrins with nucleobase substituents, that is, mono(6-ade-6-deoxy)- $\beta$ -cyclodextrin (**2**) and mono(6-ura-6-deoxy)- $\beta$ -cyclodextrin (**3**) as well as mono(6-thy-6-deoxy)- $\beta$ -cyclodextrin (**4**), were selected as molecular receptors to investigate their conformation and inclusion complexation behaviors with some chiral molecules, that is, (+)-camphor, (–)-camphor, (+)-borneol, and (–)-borneol, by spectrophotometric and microcalorimetric titrations in aqueous phosphate buffer solution (pH 7.2) at 298.15 K. Circular dichroism and NMR studies demonstrated that these nucleobase-modified  $\beta$ -cyclodextrins adopted a co-inclusion mode upon complexation with guest molecules; that is, the originally self-included nucleobase substituents of the host did not move out from the  $\beta$ -cyclodextrin cavity, but coexisted with guest molecule in the  $\beta$ -cyclodextrin cavity upon inclusion complexation. Significantly, these nucleobase-modified  $\beta$ -cyclodextrins efficiently enhanced the molecular binding ability and the chiral recognition ability of native  $\beta$ -cyclodextrin, displaying enantioselectivity up to 3.7 for (+)-camphor/(–)-camphor pair by **2** and 3.5 for (–)-borneol/(+)-borneol pair by **3**. The enhanced molecular/chiral recognition abilities of **2–4** toward ( $\pm$ )-camphor were mainly attributed to the increased entropic gains due to the extensive desolvation effects, while the favorable enthalpic gains originating from the good size-fit relationship as well as the hydrogen bond interactions between host and guest result in the enhanced molecular/chiral recognition abilities of **2–4** toward ( $\pm$ )-borneol.

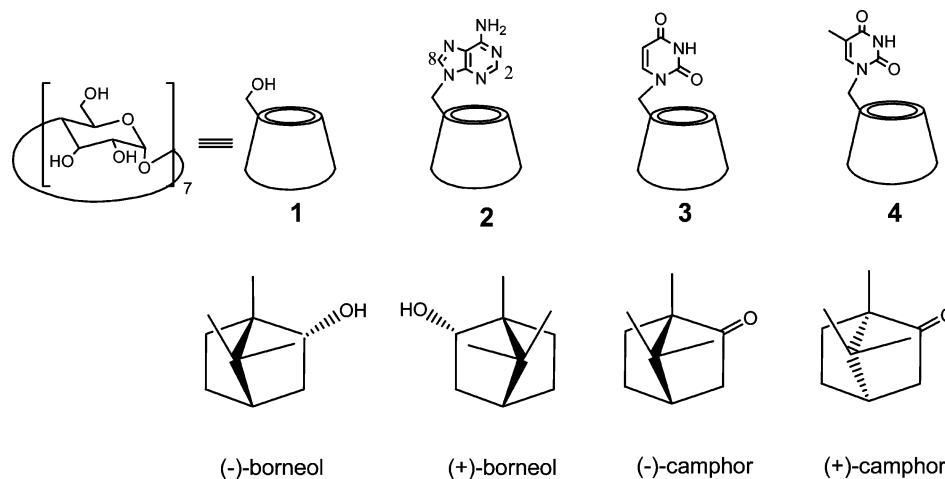
## Introduction

Possessing chiral hydrophobic cavities, cyclodextrins (CDs), a class of cyclic oligosaccharides mainly with six to eight D-glucose units linked by  $\alpha$ -1,4-glucose bonds, have been widely employed as important molecular receptors to recognize chiral guests<sup>1–5</sup> and successfully applied in chiral separation technologies.<sup>5b,6</sup> Generally, native CDs do not show fine selectivity toward many enantiomeric pairs of guests owing to the symmetrical distribution of chiral centers in the CD cavity, and the differences of  $\Delta G$  values ( $\Delta\Delta G$ ) for their complexation with guest enantiomers are basically less than 1 kJ·mol<sup>–1</sup>.<sup>7,8</sup> Superior to native CDs, modified CDs can exhibit significantly enhanced chiral recognition abilities.<sup>1d,9,10</sup> For example, mono- and diaminated  $\beta$ -CDs discriminated a wide variety of chiral guest pairs much better than native  $\beta$ -CD because of both the reduced molecular symmetry of the  $\beta$ -CD cavity and the electrostatic and/or hydrogen bond interactions between host and guest.<sup>3c,11</sup> Moreover, functional CDs have many applications as molecular receptors or drug carriers.<sup>12</sup> For example, Inoue et al. utilized  $\gamma$ -CD derivatives as chiral hosts for mediating the enantiodifferentiating photocyclodimerization of 2-anthracenecarboxylic acid. Their research results showed that  $\gamma$ -CD derivatives possessing various functional substituents brought different chemical and optical yields of chiral dimers.<sup>13</sup> Yang and co-workers achieved highly efficient separation results when using hydroxypropyl- $\beta$ -CD as chiral selector in capillary electrophoresis on the enantiomeric separation of four fluoroquinolone antimicrobial agents.<sup>14</sup> On the other hand, nucleosides and nucleobases are known to possess many important biological

activities. For example, drugs can achieve the targeted molecular therapy through their interactions with nucleobases or nucleosides.<sup>15,16</sup> Nagai et al. prepared some nucleobase-functionalized/difunctionalized  $\beta$ -CDs as nucleoside analogues, where nucleobases were attached to the C-6 positions of  $\beta$ -CD directly or through the linkage of flexible carbon chains, and investigated their pH-dependent binding abilities toward some achiral guest molecules by UV and/or circular dichroism spectroscopy.<sup>17</sup> Djedaini-Pilard et al. investigated the complexation of a nucleobase-functionalized CD with ellipticine through NMR experiments. Their results showed that  $\pi$ – $\pi$  interaction between host and guest improved the stability of the complex and resulted in increased solubility of ellipticine ultimately.<sup>18</sup> Recently, we reported the fluorescence sensing and inclusion complexation behaviors of *N,N'*-bis(2-(2-aminoethylamino)ethyl) malonamide-bridged bis( $\beta$ -CD) toward adenine and its analogues, which demonstrated that the  $\beta$ -CD cavity could efficiently include nucleobases.<sup>19</sup> However, to the best of our knowledge, the chiral recognition behaviors of nucleobase-modified  $\beta$ -CDs have not been reported. In the present work, we report the synthesis of a series of nucleobase-modified  $\beta$ -CDs and their binding behaviors as well as chiral recognition thermodynamics toward camphor and borneol enantiomers (Chart 1), both of which are bicyclic terpenoids possessing important biological functions such as antibacterial, antispasmodic, choleric, and tranquilizing effects.<sup>20</sup> There are some inherent advantages for choosing nucleobase-modified  $\beta$ -CDs as molecular receptors to recognize these chiral drugs. (1) CD cavities are able to associate with camphor and borneol to form stable host–guest inclusion complexes.<sup>4b,21,22</sup> (2) The introduction of nucleobase substituent can destroy the original symmetry of the CD cavity and thus enhance the chiral discrimination ability. (3) The nucleobase

\* Corresponding author. E-mail: yuliu@nankai.edu.cn.

## CHART 1



substituent can provide the additional binding interactions with the guest drugs accommodated in the CD cavity. It is our special interest to examine the driving force and controlling factors governing the molecular recognition behaviors of nucleobase-modified  $\beta$ -CDs from the viewpoint of thermodynamics, especially the cooperative contributions of nucleobase substituents and  $\beta$ -CD cavity to the chiral recognition, which will serve our further understanding of this recently developing, but thermodynamically less investigated, area of supramolecular chemistry.

### Experimental Section

**General.**  $\beta$ -CD of reagent grade was recrystallized twice from water and dried in vacuum at 100 °C for 24 h before use. ( $\pm$ )-Camphor and ( $\pm$ )-borneol were purchased from Aldrich or Tokyo Kasei and used as received. Adenine, uracil, and thymine were commercially available from Amresco Inc. and used without further purification. Mono[6-*O*-(*p*-toluenesulfonyl)]- $\beta$ -CD (6-OTs- $\beta$ -CD) was prepared by the reaction of  $\beta$ -CD with *p*-toluenesulfonyl chloride in aqueous alkaline solution.<sup>23</sup> Mono(6-thy-6-deoxy)- $\beta$ -CD (**4**) was prepared according to a reported procedure.<sup>17b</sup> Disodium hydrogen phosphate and sodium dihydrogen phosphate were dissolved in distilled, deionized water to make a 0.1 mol·dm<sup>-3</sup> phosphate buffer solution of pH 7.2, which was used as solvent in spectrophotometric and microcalorimetric titrations. Elemental analyses were performed on a Perkin-Elmer 2400C instrument. <sup>1</sup>H NMR spectra were recorded on a Varian Mercury Plus 400 or a Bruker AV300 instrument. 2D rotating frame Overhauser effect spectroscopy (ROESY) spectra were recorded on a Varian Mercury VX300 instrument with a mixing time of 300 ms. Mass spectra were performed on a ThermoFinnigan LCQ Advantage LC-MS, and the electrospray ionization was used. UV-vis and circular dichroism spectra were performed on a Shimadzu UV 2401 spectrophotometer and a JASCO J-715S spectropolarimeter, respectively.

**Synthesis of Mono(6-ade-6-deoxy)- $\beta$ -CD (**2**).** Anhydrous K<sub>2</sub>CO<sub>3</sub> (0.21 g, 1.52 mmol) was added to a solution of adenine (0.20 g, 1.52 mmol) and 6-OTs- $\beta$ -CD (1.30 g, 1 mmol) in dry DMF (60 mL). The mixture was heated at 80 °C for 24 h under nitrogen atmosphere. Then, the unreacted K<sub>2</sub>CO<sub>3</sub> was removed by filtration, and the filtrate was evaporated under a reduced pressure to dryness. The residue was dissolved in water, and the aqueous solution was poured into vigorously stirred acetone (300 mL) to give a slight yellow precipitate. Such an operation was repeated twice. The crude product obtained was dried in

vacuum and purified by column chromatography over Sephadex G-25 with distilled deionized water as an eluent to give **2** in 55% yield. ESI-MS *m/z* (relative intensity) 1296.14 (M + HCOO<sup>-</sup>, 100%), 1250.48 (M - H<sup>+</sup>, 95%); <sup>1</sup>H NMR (D<sub>2</sub>O):  $\delta$  3.00–3.80 (m, 42H), 4.86 (s, 7H), 7.92 (s, 1H), 7.95 (s, 1H). Anal. Calcd for C<sub>47</sub>H<sub>73</sub>N<sub>5</sub>O<sub>34</sub>·3H<sub>2</sub>O: C, 43.22; N, 5.36; H, 6.10. Found: C, 43.15; N, 5.46; H, 6.15. UV-vis  $\lambda_{\max}$  ( $\epsilon$ ): 261 nm (1.13 × 10<sup>4</sup> M<sup>-1</sup> cm<sup>-1</sup>).

**Synthesis of Mono(6-ura-6-deoxy)- $\beta$ -CD (**3**).** Compound **3** was prepared in 50% yield from uracil and 6-OTs- $\beta$ -CD according to the procedure similar to that in the synthesis of **2**. ESI-MS *m/z* (relative intensity) 1263.30 (M + Cl<sup>-</sup>, 100%), 1227.40 (M - H<sup>+</sup>, 60%); <sup>1</sup>H NMR (D<sub>2</sub>O):  $\delta$  3.47–3.91 (m, 42H), 4.94–5.05 (m, 7H), 5.76 (d, 1H, *J* = 7.8 Hz), 7.53 (d, 1H, *J* = 7.8 Hz). Anal. Calcd for C<sub>46</sub>H<sub>72</sub>N<sub>2</sub>O<sub>36</sub>·4H<sub>2</sub>O: C, 42.46; N, 2.15; H, 6.20. Found: C, 42.35; N, 2.23; H, 6.08. UV-vis  $\lambda_{\max}$  ( $\epsilon$ ): 265.4 nm (4.70 × 10<sup>3</sup> M<sup>-1</sup> cm<sup>-1</sup>).

**Microcalorimetry.** The thermodynamic parameters were determined at atmospheric pressure in aqueous phosphate buffer solution (pH 7.2) at 25 °C by using a Microcal VP-ITC titration microcalorimeter, which allows us to determine simultaneously the enthalpy and equilibrium constant from a single titration curve. The VP-ITC instrument was calibrated chemically by performing a complexation reaction of  $\beta$ -CD with cyclohexanol, and the thermodynamic parameters obtained were shown to be in good agreement with literature data.<sup>24</sup> All solutions were degassed and thermostated using a ThermoVac accessory before each titration run. In each run, a phosphate buffer solution of host in a 250- $\mu$ L syringe was sequentially injected with stirring at 300 rpm into a buffer solution of guest in the calorimeter's sample cell. The sample volume was 1.4227 mL in all experiments. Each titration experiment was composed of 25 successive injections (10  $\mu$ L per injection). A typical titration curve is shown in Figure 1. Each titration of host CDs into the sample cell gave rise to a heat of reaction, caused by the formation of inclusion complexes between guest molecules and host CDs. The heats of reaction decreased after each injection of host CDs because fewer and fewer guest molecules were available to form inclusion complexes. A control experiment was performed to determine the heat of dilution by injecting a host solution into a pure buffer solution containing no guest molecules. The dilution heat determined in the control experiment was subtracted from the apparent reaction heat measured in the titration experiments to give the net reaction heat.

The net reaction heat in each run was analyzed by using "one set of binding sites" model (Origin software, Microcal Inc.) to

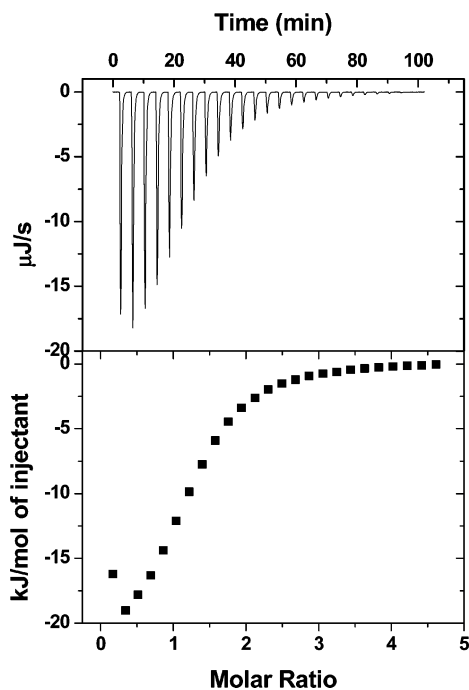


**Figure 1.** Calorimetric titration curve of **2** with (+)-borneol in phosphate buffer solution (pH 7.2) at 25 °C. (Upper) Raw data for sequential 10- $\mu$ L injections of **2** solution (3.38 mM) into (+)-borneol solution (0.14 mM). (Lower) Heats of reactions as obtained from the integration of the calorimetric traces.

simultaneously compute the binding stoichiometry ( $N$ ), complex stability constant ( $K_s$ ), standard molar reaction enthalpy ( $\Delta H^\circ$ ), and standard deviation from the titration curve. The knowledge of complex stability constant ( $K_s$ ) and molar reaction enthalpy ( $\Delta H^\circ$ ) enabled the calculation of standard free energy ( $\Delta G^\circ$ ) and entropy changes ( $\Delta S^\circ$ ). A typical curve fitting result for the complexation of **4** with (-)-camphor was shown in Figure 2. To check the accuracy of observed thermodynamic parameters, at least two independent titration experiments were carried out to afford self-consistent thermodynamic parameters, and their average values were listed in Table 1.

## Results and Discussion

**Synthesis.** Nucleobase-modified  $\beta$ -CDs were synthesized in satisfactory yield by the reactions of 6-OTs- $\beta$ -CD with corresponding nucleobases. All the reactions were carried out in DMF solution, which avoided the formation of inclusion complexes between the nucleobases and  $\beta$ -CD cavity because CD cavities barely include guest molecules in DMF solution.<sup>25</sup> Moreover, the ESI-MS data clearly demonstrate the connectivity of nucleobase substituents with  $\beta$ -CD cavity.

**Circular Dichroism Spectroscopy.** Circular dichroism spectrometry is a convenient and widely employed method to elucidate the conformation of the CD-containing system. Generally, if an achiral chromophore is enclosed in or adjacent to the chiral CD cavity, it will give either positive or negative induced circular dichroism (ICD) signals according to the location and orientation of transition dipole moment of chromophore with respect to the CD axis. For the chromophore located inside the CD cavity or perched on the edge of the CD cavity, its electronic transition parallel to the CD axis gives a positive ICD signal, whereas perpendicular transition gives a negative signal.<sup>26</sup> As can be seen in Figure 3, the circular dichroism spectrum of **2** displays a strong negative Cotton effect peak at 261 nm ( $\Delta\epsilon = -6.86 \text{ M}^{-1} \text{ cm}^{-1}$ ) and a moderate positive Cotton effect peak

at 209 nm ( $\Delta\epsilon = +4.76 \text{ M}^{-1} \text{ cm}^{-1}$ ) assigned to the  $^1L_a$  and  $^1L_b$  transitions of adenine substituent, respectively. Therefore, we can deduce that the adenine substituent is deeply self-included into the  $\beta$ -CD cavity as illustrated in Chart 2, where its  $^1L_a$  transition is nearly parallel, while its  $^1L_b$  transition is nearly perpendicular, to the  $C_7$  axis of  $\beta$ -CD cavity. In contrast, hosts **3** and **4** have ICD signals obviously different from that of **2**. The circular dichroism spectrum of **3** displays a weak negative Cotton effect peak at 218 nm ( $\Delta\epsilon = -1.09 \text{ M}^{-1} \text{ cm}^{-1}$ ) and a strong positive Cotton effect peak at 268 nm ( $\Delta\epsilon = +8.97 \text{ M}^{-1} \text{ cm}^{-1}$ ) assigned to the  $^1L_a$  and  $^1L_b$  transitions of the uracil substituent, respectively. Similarly, the circular dichroism spectrum of **4** displays a weak negative Cotton effect peak at 234 nm ( $\Delta\epsilon = -0.78 \text{ M}^{-1} \text{ cm}^{-1}$ ) and a strong positive Cotton effect peak at 270 nm ( $\Delta\epsilon = +6.27 \text{ M}^{-1} \text{ cm}^{-1}$ ) assigned to the  $^1L_a$  and  $^1L_b$  transitions of the thymine substituent, respectively. These ICD signals indicate that the substituent group of **3** or **4** is shallowly self-included in the  $\beta$ -CD cavity with a tilt-in conformation, where its  $^1L_a$  transition is nearly perpendicular, while its  $^1L_b$  transition is nearly parallel, to the  $C_7$  axis of  $\beta$ -CD cavity (Chart 2). Moreover, by comparing the ICD signals of **3** and **4**, we may find that **3** ( $\Delta\epsilon = +8.97 \text{ M}^{-1} \text{ cm}^{-1}$ ) gives a Cotton effect peak stronger than that of **4** ( $\Delta\epsilon = +6.27 \text{ M}^{-1} \text{ cm}^{-1}$ ), although they possess quite similar structures. A possible reason is that the uracil group of **3** enters the  $\beta$ -CD cavity more deeply than the thymine group of **4** does. These ICD signals of **2–4** are consistent with the reported ones with a self-included conformation.<sup>17b,d,22b,27,28</sup>

Upon inclusion complexation with guest molecules, the ICD signals of **2–4** retain their original shapes, but their Cotton effect intensities show different changes. This implies that the nucleobase substituents of **2–4** are still located in the  $\beta$ -CD cavity, but their self-inclusion depth changes in different degrees after inclusion. As seen in Figure 4, with the addition of (-)-borneol, the negative Cotton effect intensity of **2** decreases to  $\Delta\epsilon = -5.96 \text{ M}^{-1} \text{ cm}^{-1}$  (255 nm), while the positive one reduces to  $4.32 \text{ M}^{-1} \text{ cm}^{-1}$  (208 nm). However, the positive Cotton effect intensities of **3** and **4** increase to  $\Delta\epsilon = +11.19 \text{ M}^{-1} \text{ cm}^{-1}$  (268 nm) for **3** and  $+10.00 \text{ M}^{-1} \text{ cm}^{-1}$  (270 nm) for **4**, while the negative one is enhanced to  $\Delta\epsilon = -1.55 \text{ M}^{-1} \text{ cm}^{-1}$  (218 nm) for **3** and  $-1.40 \text{ M}^{-1} \text{ cm}^{-1}$  (238 nm) for **4**, respectively. These phenomena indicate that the self-included adenine substituent of **2** is partly expelled from the  $\beta$ -CD cavity, but the uracil or thymine substituents of **3** or **4** move more deeply into the  $\beta$ -CD cavity, after complexation with guest molecules. That is to say, the nucleobase-modified  $\beta$ -CDs can adjust their conformation upon inclusion complexation with guest molecules. Similar ICD results are also observed in the cases of inclusion complexation of **2–4** with other guests of camphor and borneol.

**NMR Spectra.**  $^1\text{H}$  NMR investigations give further information about the conformation of hosts **2–4** in the absence and presence of guest molecules. As seen in Figure 5a, the  $^1\text{H}$  NMR spectrum of free adenine shows two NMR signals at  $\delta$  8.00 and 8.05 assigned to the H2 and H8 protons, respectively. After the adenine group attaches to the  $\beta$ -CD rim, the two resonance signals shift upfield to  $\delta$  7.93 and 7.95, respectively, which is attributed to the formation of the covalent bond changing the electron density of the adenine ring as well as the changes of magnetic field around the adenine group induced by the hydrophobic microenvironment of the  $\beta$ -CD cavity. Interestingly, these signals show further upfield shifts after complexation with guest molecules (Figure 5c,d), indicating that the adenine group is still located in the  $\beta$ -CD cavity and interacts with the included guest molecule. By comparing the  $\Delta\delta$  values

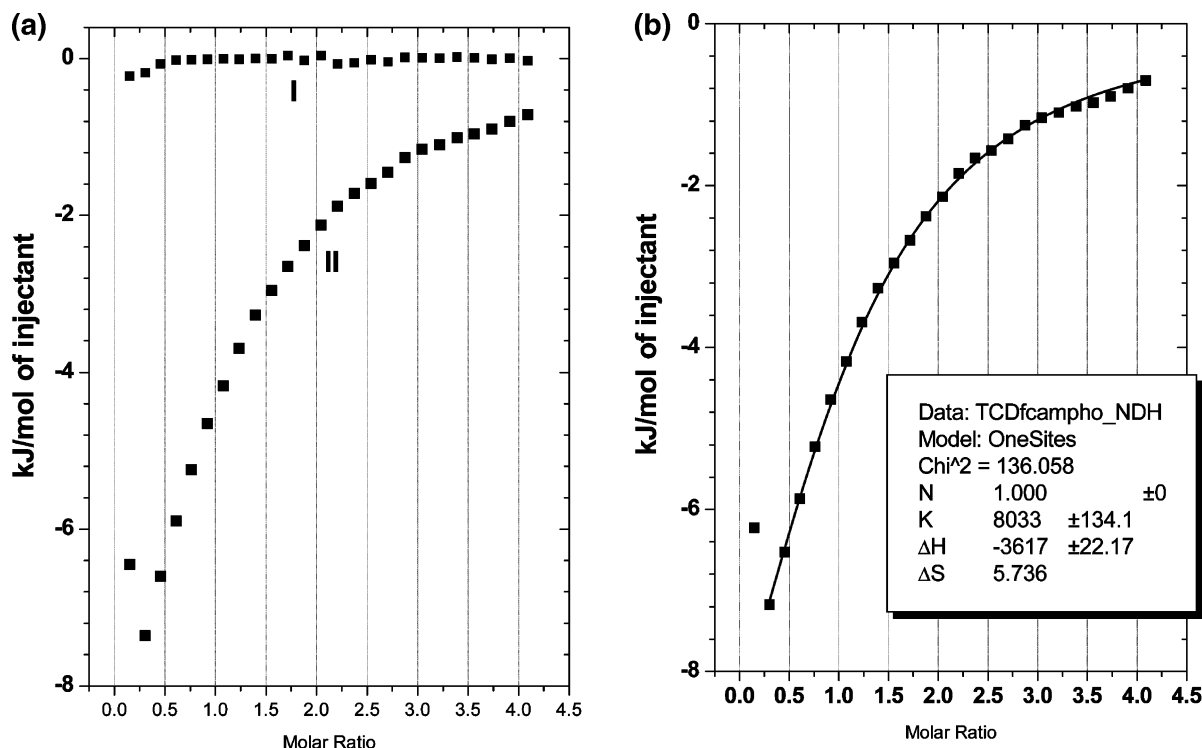


**Figure 2.** (a) Heat effects of dilutions (I) and of complexation (II) of **4** with (–)-camphor for each injection during titration microcalorimetric experiment. (b) “Net” heat effect obtained by subtracting the heat of dilution from the heat of reaction, which was analyzed by computer simulation using the “one set of binding sites” mode.

**TABLE 1: Complex Stability Constant ( $K_s$ ) and Thermodynamic Parameters for 1:1 Complexation of (±)-Camphor and (±)-Borneol with Hosts 1–4 in Phosphate Buffer Solution (pH 7.2) at 298.15 K<sup>a</sup>**

hosts	guests	$K_s$ (M <sup>-1</sup> )	$\Delta G^\circ$ (kJ·mol <sup>-1</sup> )	$\Delta H^\circ$ (kJ·mol <sup>-1</sup> )	$T\Delta S^\circ$ (kJ·mol <sup>-1</sup> )
1 <sup>b</sup>	(+)-camphor	8261 ± 261	-22.4 ± 0.1	-13.8 ± 0.5	8.5 ± 0.6
	(-)-camphor	4988 ± 60	-21.1 ± 0.1	-23.8 ± 0.6	-2.7 ± 0.6
	(+)-borneol	18640 ± 110	-24.4 ± 0.1	-20.9 ± 0.5	3.5 ± 0.6
	(-)-borneol	19750 ± 580	-24.5 ± 0.1	-23.2 ± 0.1	1.3 ± 0.2
2 <sup>c</sup>	(+)-camphor	48180 ± 1050	-26.7 ± 0.1	-13.5 ± 0.2	13.2 ± 0.1
	(-)-camphor	13040 ± 480	-23.5 ± 0.1	-17.1 ± 0.2	6.4 ± 0.1
	(+)-borneol	51000 ± 950	-26.9 ± 0.1	-28.9 ± 0.1	-2.0 ± 0.2
	(-)-borneol	86670 ± 1070	-28.2 ± 0.1	-30.9 ± 0.1	-2.7 ± 0.1
3 <sup>c</sup>	(+)-camphor	16020 ± 480	-24.0 ± 0.1	-12.9 ± 0.2	11.1 ± 0.2
	(-)-camphor	12660 ± 420	-23.4 ± 0.1	-14.9 ± 0.2	8.5 ± 0.3
	(+)-borneol	19300 ± 730	-24.5 ± 0.1	-28.2 ± 0.1	-3.7 ± 0.2
	(-)-borneol	67520 ± 1070	-27.6 ± 0.1	-30.9 ± 0.1	-3.3 ± 0.1
4 <sup>c</sup>	(+)-camphor	8930 ± 60	-22.6 ± 0.1	-14.2 ± 0.1	8.4 ± 0.1
	(-)-camphor	8050 ± 17	-22.3 ± 0.0	-15.1 ± 0.1	7.2 ± 0.1
	(+)-borneol	33780 ± 720	-25.8 ± 0.1	-28.5 ± 0.1	-2.7 ± 0.2
	(-)-borneol	35150 ± 370	-25.9 ± 0.1	-30.2 ± 0.1	-4.3 ± 0.1

<sup>a</sup> [Host] = 3.00–3.38 mM. [Guest] = 0.13–0.14 mM. <sup>b</sup> Reference 4b. <sup>c</sup> This work.

of adenine protons in **2** (Table 2), we deduce that the adenine protons have bigger upfield shifts upon complexation with borneol than those with camphor. This phenomenon may indicate the stronger interactions between the adenine group in **2** with the borneol guest, which is consistent with the results of microcalorimetric titrations as described later.

Two-dimensional NMR spectroscopy is an essential method for the conformational studies of CDs and their complexes since one can conclude that two protons are closely located in space if an NOE correlation is detected between the relevant proton signals in the NOESY or ROESY spectrum. Therefore, it is possible to estimate the orientation of the substituent moiety or guest molecule in the CD cavity by using the assigned NOE correlations. As seen in Figure 6a, the ROESY spectrum of **2** shows clear NOE correlations (peak A) between the adenine proton of **2** and the interior protons (H3/H5) of  $\beta$ -CD cavity,

indicating that the adenine substituent is self-included into the  $\beta$ -CD cavity. Further comparison shows that the adenine proton has stronger NOE correlations with the H3 protons than those with H5 protons of  $\beta$ -CD. Because the H5 protons are located at the narrow side, while the H3 protons are at the wide side, of the  $\beta$ -CD cavity, these NOE correlations demonstrate that the adenine substituent is deeply self-included in the  $\beta$ -CD cavity. Interestingly, the ROESY spectrum of an equimolar mixture of **2** with (–)-borneol (Figure 6b) also presents NOE correlations (peak A) between the adenine proton of **2** and the interior protons of the  $\beta$ -CD cavity, but the strength of NOE correlations of the adenine proton of **2** with  $\beta$ -CD's H5 protons becomes stronger than that with  $\beta$ -CD's H3 protons. This indicates that the adenine substituent of **2** is still located in the  $\beta$ -CD cavity and partly moves to the narrow side. Moreover, the (–)-borneol protons give NOE correlations with both the

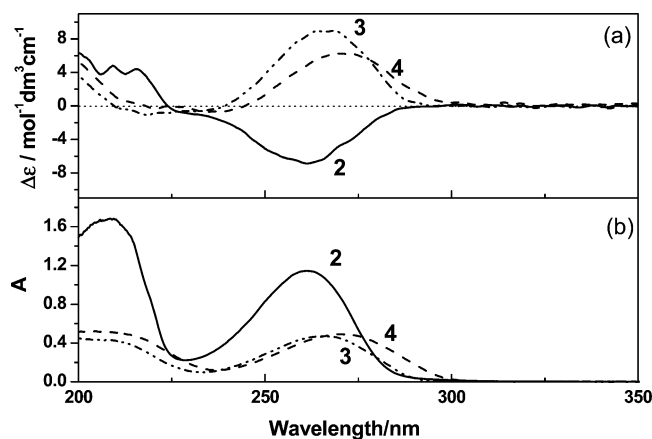


**Figure 3.** Circular dichroism (a) and absorption (b) spectra of **2–4** ( $1.0 \times 10^{-4}$  M) in aqueous phosphate buffer solution (pH 7.2) at 25 °C.

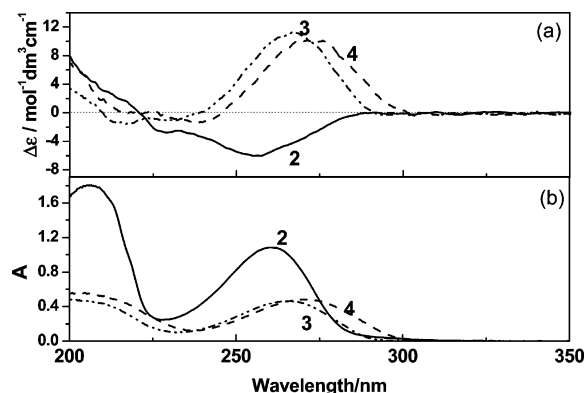


**Figure 4.** Circular dichroism (a) and absorption (b) spectra of **2–4** ( $1.0 \times 10^{-4}$  M) in the presence of (–)-borneol in aqueous phosphate buffer solution (pH 7.2) at 25 °C.

adenine proton of **2** (peak B) and the interior protons of  $\beta$ -CD cavity (peaks C, D, E, F, G, H). Among them, peak B is assigned to the NOE correlations between  $H_g$  protons of (–)-borneol and the adenine proton of **2**. Peak C is assigned to the NOE correlations between  $H_g$  protons of (–)-borneol and H3/H5 protons of  $\beta$ -CD, where the  $H_g$  protons show stronger NOE correlations with H3 protons than those with H5 protons of  $\beta$ -CD. Peak D is assigned to the NOE correlations between the  $H_h$  protons of (–)-borneol and the H5 protons of  $\beta$ -CD; Peaks E and G are assigned to the NOE correlations of the  $H_c/H_d$  protons of (–)-borneol with the H3/H5 protons of  $\beta$ -CD. Peak F is assigned to the NOE correlations of the  $H_e$  protons of (–)-borneol with the H3 protons of  $\beta$ -CD. Peak H is assigned to the NOE correlations of the  $H_a/H_b$  protons of (–)-borneol with the H3/H5 protons of  $\beta$ -CD, where the H3 protons show NOE correlations stronger than those of the H5 protons. Moreover, the NOE correlation of the  $H_f$  proton of (–)-borneol with the adenine protons of **2** may be overlapped with peak A, which makes it difficult to be clearly assigned. Even so, we can also deduce a possible binding mode of **2** with (–)-borneol as illustrated in Figure 6c according to the assigned NOE cross-peaks A–H. This binding mode is further supported by a Corey–Pauling–Koltun (CPK) molecular modeling study. The results show that both the adenine substituent of **2** and the guest molecule (–)-borneol coexist in the  $\beta$ -CD cavity upon inclusion as illustrated in Figure 6d, which is in good agreement with the one deduced from the circular dichroism spectral studies.

**Binding Stoichiometry.** It is widely reported that CDs mainly form 1:1 inclusion complexes with model substrates. In our

experiments, the titration data also give the 1:1 binding stoichiometry between host and guest with “ $N$ ” values in the curve fitting results varying from 0.9 to 1.1. Moreover, the CPK molecular modeling study demonstrates that hosts **2–4** can only accommodate one camphor or borneol in its hydrophobic cavity, which subsequently rationalizes the 1:1 binding stoichiometry between host and guest. Therefore, a fixed 1:1 binding stoichiometry is used in the curve-fitting analysis of calorimetric titration.

**Binding Ability.** It is well-known that the induced-fit interactions between host and guest play an important role in the inclusion course, and the binding ability mainly depends on the fitting efficiency of the size, shape, and functional group of a guest into those of a CD host.<sup>29</sup> A high fitting efficiency usually leads to not only the strong van der Waals and hydrophobic interactions whose strength is closely related to the distance and contact surface area between the CD cavity and the accommodated guest, but also the strong electrostatic and/or hydrogen bond interactions between the substituent of CD host and the functional group of guest molecule. As can be seen in Table 1, all of the nucleobase-modified  $\beta$ -CDs **2–4** exhibit stronger binding abilities toward camphor and borneol than native  $\beta$ -CD. For example, the stability constants ( $K_s$ ) for the inclusion complexation of hosts **2–4** toward camphor are 1.08–5.83 times, while those toward borneol are 1.04–4.39 times, higher than the corresponding values for the inclusion complexation of native  $\beta$ -CD. Circular dichroism and NMR studies have demonstrated that all of the hosts **2–4** adopt the self-included conformation in aqueous solution. This conformation inevitably decreases the effective volume of  $\beta$ -CD cavity to some extent, which consequently leads to the higher size-fit efficiency between host and guest. Moreover, the molecular modeling studies demonstrated that there exist the effective hydrogen bond interactions between the carbonyl (for camphor) or the hydroxyl (for borneol) group of guest molecule and the nucleobase substituents of hosts **2–4** (Figure 6d), which also contributes to the strong host–guest binding. As a joint result of these two factors, hosts **2–4** have stronger binding abilities than native  $\beta$ -CD. A close comparison on the binding abilities of **2–4** shows that host **2** gives the highest complex stability constants toward the examined guest molecules. A possible reason is that the adenine substituent of **2** is self-included into the  $\beta$ -CD cavity more deeply than the uracil or thymine substituent of **3** or **4**, as estimated from the circular dichroism signals. This deep self-included conformation leads to the smallest effective volume of  $\beta$ -CD cavity among the examined nucleobase-modified  $\beta$ -CDs and thus the best size-fit efficiency between host and guest.

From Table 1, we can also find that all of the hosts **1–4** have stronger binding abilities toward borneol than toward camphor. A comparison of their structures shows that camphor and borneol present only a small difference in the structure of C-2 substituent; that is, a carbonyl group for camphor and a hydroxyl group for borneol. However, this slight difference will lead to the great distinction in their binding abilities with host CDs. NMR studies have demonstrated that the C-2 substituent of guest is located close to the self-included nucleobase substituent of host. This close location in space consequently leads to the additional hydrogen bond interactions between host and guest. Possessing a hydroxyl group at the C-2 position, borneol can give the strong hydrogen bond interactions with the nucleobase substituents as well as the numerous hydroxyl groups of host CDs. In contrast, possessing a hydrophobic carbonyl group at the C-2 position, camphor can give only the

## CHART 2: Possible Conformation of 2–4

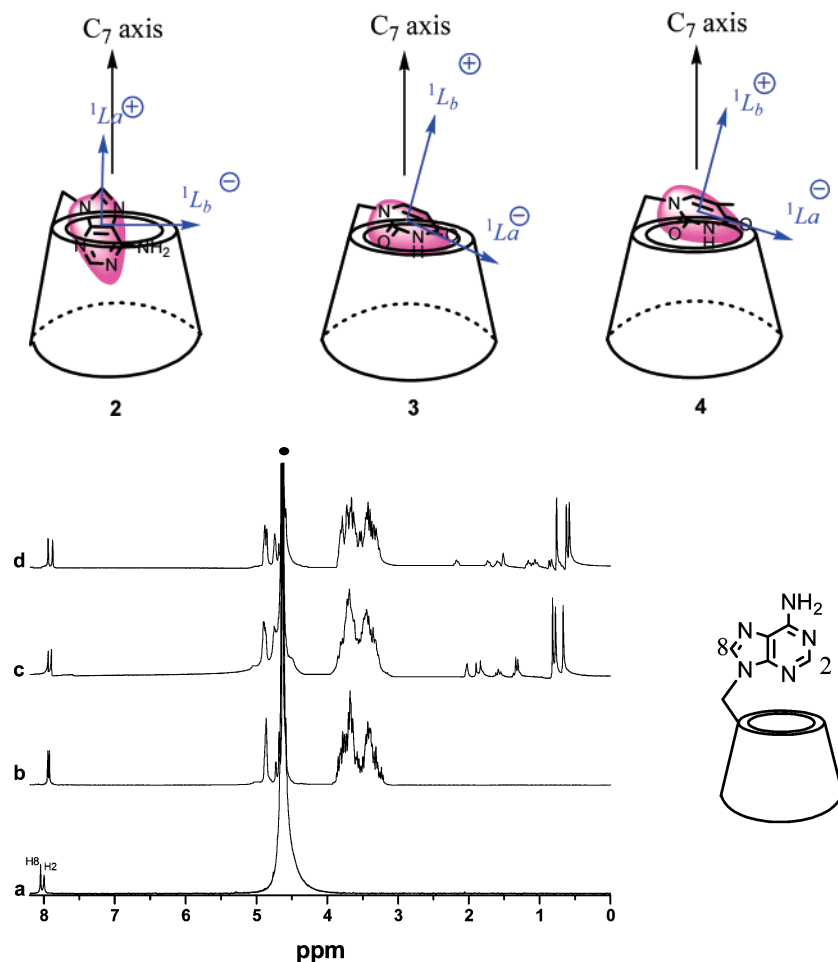


**Figure 5.**  $^1\text{H}$  NMR spectra of (a) free adenine, (b) **2**, (c) **2** + (+)-camphor, and (d) **2** + (+)-borneol in  $\text{D}_2\text{O}$  at  $25\text{ }^\circ\text{C}$ . ( $[\mathbf{2}] = [(\text{+})\text{-borneol}] = [(\text{+})\text{-camphor}] = 2 \times 10^{-3}\text{ M}$ .) Symbol  $\bullet$  indicates the solvent, which is identified at 4.634 ppm.

**TABLE 2: Chemical Shifts ( $\delta$ ) of H2 and H8 Protons in Adenine, **2**, 2-(+)-Borneol, and 2-(+)-Camphor in  $\text{D}_2\text{O}$  at  $25\text{ }^\circ\text{C}$**

	$\delta$ (ppm)			
	adenine	<b>2</b>	2-(+)-camphor	2-(+)-borneol
H <sub>8</sub>	8.05	7.95	7.94	7.94
H <sub>2</sub>	8.00	7.93	7.90	7.88

relatively weak hydrogen bond interactions with host CDs, which consequently results in its lower binding abilities with **1–4** than borneol.

**Thermodynamic Parameters.** It is well documented that, among several weak noncovalent interactions working between CD and guest, the hydrogen bond and van der Waals interactions between host and guest mainly contribute to the enthalpic changes, while the desolvation effect and the conformation change cause the entropic changes.<sup>30</sup> As can be readily recognized from Table 1, all of the associations of hosts **2–4** with camphor and borneol give negative enthalpic changes ( $\Delta H^\circ < 0$ ), accompanied by either the positive (for camphor,  $T\Delta S^\circ > 0$ ) or negative (for borneol,  $T\Delta S^\circ < 0$ ) entropic changes. These results indicate that the hydrogen bond and van der Waals interactions are the main driving forces of the associations of hosts **2–4**. On the other hand, the relatively complicated entropic changes can be analyzed from the facets of both the conformation fixation and the desolvation effect upon host–guest complexation. A close comparison shows that the associations of hosts **2–4** with borneol display more negative

enthalpic changes ( $-28.2$  to  $-30.9\text{ kJ}\cdot\text{mol}^{-1}$ ) than those with camphor ( $-12.9$  to  $-17.1\text{ kJ}\cdot\text{mol}^{-1}$ ), which confirms stronger hydrogen bond interactions between hosts **2–4** and borneol from the thermodynamic viewpoint. It is also interesting to compare the entropic changes of the associations of hosts **2–4** with camphor and borneol. Generally, the association process, which leads to the loss of conformational freedom, is inherently accompanied by the entropic loss. On the other hand, before association, both the free host CD and the free guest molecule are solvated, and the solvent molecules around the host and the guest are highly ordered. During the association, both the host and the guest have to lose their solvation shell. This process causes the disorder of system to increase and thus leads to a favorable entropy gain, which compensates the entropic loss arising from the loss of conformational freedom upon association in different degrees. Therefore, we can deduce that the strong binding of hosts **2–4** with borneol leads to the large entropic loss, which entirely overwhelms the entropic gain from the desolvation effect and thus results in the negative total entropic changes. However, camphor can exclude more water molecules from the  $\beta$ -CD cavity upon association because of its higher hydrophobicity. This extensive desolvation process is inherently accompanied by the larger entropic gain, which subsequently compensates the lower entropic loss from the relatively weak binding of camphor with hosts **2–4**. Thus, camphor gives the positive total entropic changes upon complexation with hosts **2–4**.

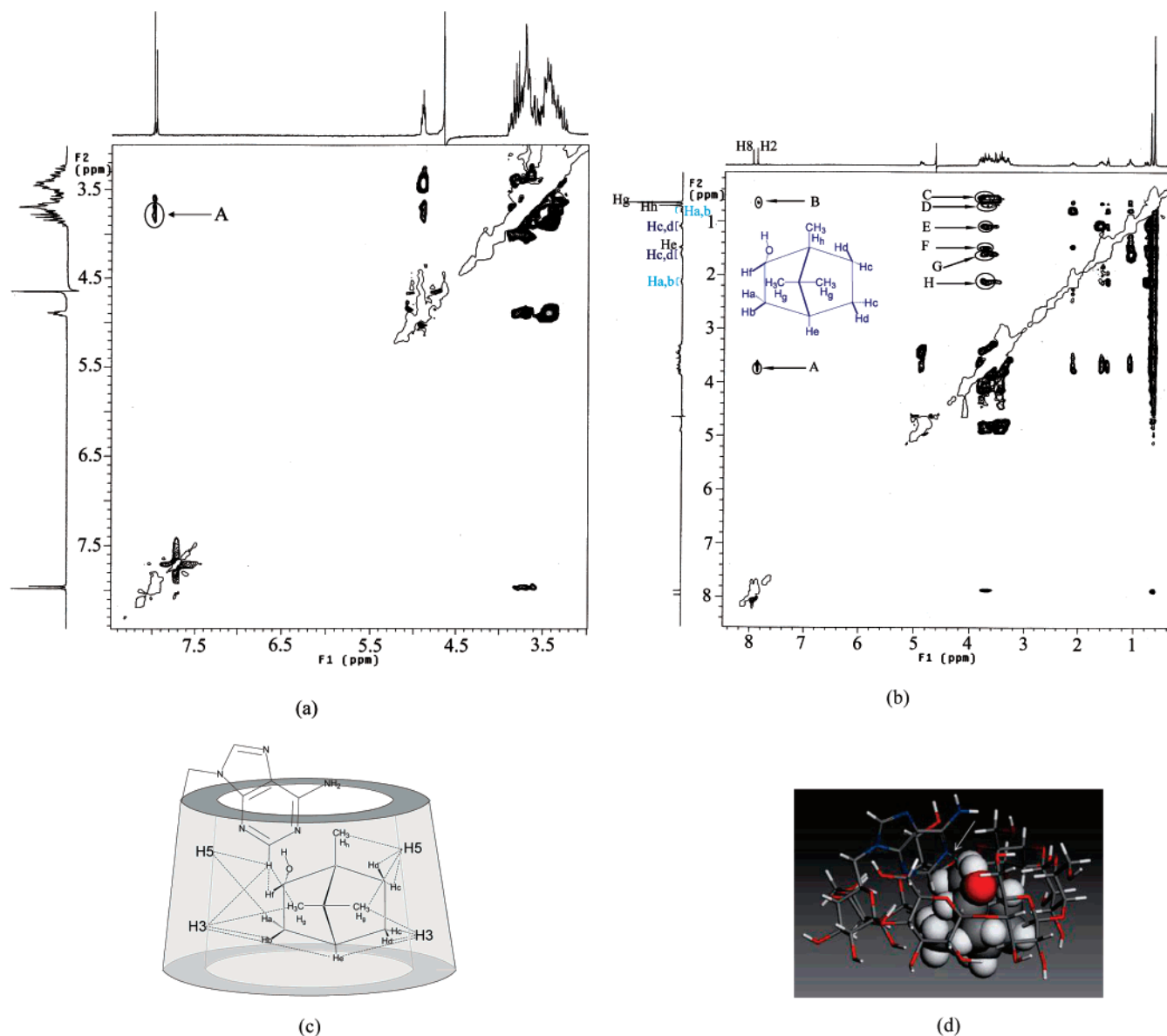


**Figure 6.** ROESY spectra of **2** in the absence (a) and presence (b) of (-)-borneol. (c) Possible binding mode of **2** with (-)-borneol. (d) Structure of **2**/(-)-borneol based on molecular modeling study. The structure was colored by atom type: gray, carbon atoms; red, oxygen atoms; blue, nitrogen atoms; white, hydrogen atoms. Hydrogen bond between adenine substituent and (-)-borneol was marked by arrow. The hydrogen bond between adenine/borneol and cyclodextrin as well as intramolecular hydrogen bond of cyclodextrin were ignored.

Moreover, a comparison between the differential enthalpic and entropic changes for the associations of hosts **2–4** with borneol exhibits that all the differential enthalpic changes for nucleobase-CD/borneol systems ( $\Delta H^\circ_{2-4} - \Delta H^\circ_{\beta-CD} = -6.7$  to  $-8.0$   $\text{kJ}\cdot\text{mol}^{-1}$ ) are more negative than the differential entropic changes ( $T\Delta S^\circ_{2-4} - T\Delta S^\circ_{\beta-CD} = -4.0$  to  $-7.2$   $\text{kJ}\cdot\text{mol}^{-1}$ ), which means that the favorable enthalpic gains mainly contribute to the enhanced binding ability of hosts **2–4** toward borneol as compared to the native  $\beta$ -CD. On the other hand, for the associations with camphor, the calculated enthalpic and entropic changes reveal that all the differential entropic changes ( $T\Delta S^\circ_{2-4} - T\Delta S^\circ_{\beta-CD} = -0.1$  to  $11.2$   $\text{kJ}\cdot\text{mol}^{-1}$ ) for nucleobase-CD/camphor systems are more positive than the enthalpic changes ( $\Delta H^\circ_{2-4} - \Delta H^\circ_{\beta-CD} = -0.4$  to  $8.9$   $\text{kJ}\cdot\text{mol}^{-1}$ ), indicating that the enhanced binding of **2–4** toward camphor is mainly contributed from the entropic gains.

**Chiral Recognition.** In addition to the stronger binding abilities, hosts **2–4** also show higher chiral recognition abilities than native  $\beta$ -CD. As can be seen from Table 1,  $\beta$ -CD gives relatively low selectivities up to 1.66 toward (+)-camphor/

(-)-camphor pair ( $K_{S(+)-camphor}/K_{S(-)-camphor}$ ) and 1.06 toward (-)-borneol/(+)-borneol pair ( $K_{S(-)-borneol}/K_{S(+)-borneol}$ ), but this value is significantly enhanced to 3.7 toward (+)-camphor/(-)-camphor pair by **2** and 3.5 toward (-)-borneol/(+)-borneol pair by **3**. Thermodynamically, the enthalpic loss for the association of **2** with (+)-camphor is calculated as  $\Delta\Delta H^\circ_{(+)-camphor} = \Delta H^\circ_{2/(+)-camphor} - \Delta H^\circ_{\beta-CD/(+)-camphor} = 0.3$   $\text{kJ}\cdot\text{mol}^{-1}$ , which is 6.4  $\text{kJ}\cdot\text{mol}^{-1}$  smaller than that for the association of (-)-camphor with **2**,  $\Delta\Delta H^\circ_{2/(-)-camphor} = \Delta H^\circ_{2/(-)-camphor} - \Delta H^\circ_{\beta-CD/(-)-camphor} = 6.7$   $\text{kJ}\cdot\text{mol}^{-1}$ . However, the significant difference in enthalpic losses for (+)/(-)-isomers is completely compensated by the large entropic gains ( $T\Delta\Delta S^\circ_{2/(+)-camphor} = T\Delta S^\circ_{2/(+)-camphor} - T\Delta S^\circ_{\beta-CD/(+)-camphor} = 4.7$   $\text{kJ}\cdot\text{mol}^{-1}$ ;  $T\Delta\Delta S^\circ_{2/(-)-camphor} = T\Delta S^\circ_{2/(-)-camphor} - T\Delta S^\circ_{\beta-CD/(-)-camphor} = 9.1$   $\text{kJ}\cdot\text{mol}^{-1}$ ), which ultimately gives an enhancement in enantioselectivity as 3.7. These results indicate that the enhanced chiral discrimination of **2** toward ( $\pm$ )-camphor should be attributed to the increased positive entropic changes rather than the enthalpic losses. On the other hand, the entropic loss for the association of **3** with (-)-borneol is calculated as  $T\Delta\Delta S^\circ_{3/(-)-borneol}$

$= T\Delta S_{3(-)-borneol}^{\circ} - T\Delta S_{\beta-CD(-)-borneol}^{\circ} = -4.6 \text{ kJ}\cdot\text{mol}^{-1}$ , which is  $2.6 \text{ kJ}\cdot\text{mol}^{-1}$  larger than that for the association of (+)-borneol with **3**,  $T\Delta\Delta S_{3(+)-borneol}^{\circ} = -7.2 \text{ kJ}\cdot\text{mol}^{-1}$ , whereas these differences in entropic loss for (+)/(-)-isomers are also overwhelmed by the enthalpic gains ( $\Delta\Delta H_{3(-)-borneol}^{\circ} = \Delta H_{3(-)-borneol}^{\circ} - \Delta H_{\beta-CD(-)-borneol}^{\circ} = -7.7 \text{ kJ}\cdot\text{mol}^{-1}$ ;  $\Delta\Delta H_{3(+)-borneol}^{\circ} = \Delta H_{3(+)-borneol}^{\circ} - \Delta H_{\beta-CD(+)-borneol}^{\circ} = -7.3 \text{ kJ}\cdot\text{mol}^{-1}$ ). Therefore, we can deduce that the enhanced enantioselectivity of **3** toward ( $\pm$ )-borneol is attributed to the favorable enthalpic gains rather than the unfavorable entropic losses.

## Conclusion

In summary, we successfully synthesized three nucleobase-modified  $\beta$ -CDs and thermodynamically investigated their binding behaviors toward camphor and borneol. Because of the cooperative contributions of van der Waals, hydrogen bond, and hydrophobic interactions, these nucleobase-modified  $\beta$ -CDs display enhanced binding abilities and molecular/chiral selectivities as compared with those of native  $\beta$ -CD, giving enantioselectivities up to 3.7 for (+)-camphor/(-)-camphor pair and 3.5 for (-)-borneol/(+)-borneol pair. The good size-fit relationship and the extensive desolvation effect arising from the co-inclusion binding mode were found responsible for the enhanced binding abilities and molecular selectivities.

**Acknowledgment.** This work was supported by the 973 program (2006CB932900), NNSFC (20673061), Special Fund for Doctoral Program from the Ministry of Education of China (20050055004), and Tianjin Natural Science Foundation (06YFJMJC04400), which are gratefully acknowledged.

**Supporting Information Available:** Enthalpy–entropy compensation plot for the inclusion complexation of camphor/borneol guests with hosts **2–4** and the enlarged partial images of 2D NMR spectra. This material is available free of charge via the Internet at <http://pubs.acs.org>.

## References and Notes

- (1) (a) Kano, K. Selectivities in Cyclodextrin Chemistry. In *Bioorganic Chemistry Frontiers*; Dugas, H., Schmidtchen, F. P., Eds.; Springer-Verlag: Berlin, 1993; Vol. 3, Ch. 1. (b) Kano, K. *J. Phys. Org. Chem.* **1997**, *10*, 286. (c) Kano, K.; Kamo, H.; Negi, S.; Kitae, T.; Takaoka, R.; Yamaguchi, M.; Okubo, H.; Hiram, M. *J. Chem. Soc., Perkin Trans. 2* **1999**, *15*. (d) Kano, K.; Kato, Y.; Koder, M. *J. Chem. Soc., Perkin Trans. 2* **1996**, 1211. (e) Kano, K.; Hasegawa, H.; Miyamura, M. *Chirality* **2001**, *13*, 474. (f) Kano, K.; Hasegawa, H. *J. Am. Chem. Soc.* **2001**, *123*, 10616. (g) Kano, K.; Yoshiyasu, K.; Hashimoto, S. *J. Chem. Soc., Chem. Commun.* **1989**, 1278.
- (2) (a) Kean, S. D.; May, B. L.; Clements, P.; Lincoln, S. F.; Easton, C. J. *J. Chem. Soc., Perkin Trans. 2* **1999**, 1257. (b) Haskard, C. A.; Easton, C. J.; May, B. L.; Lincoln, S. F. *Inorg. Chem.* **1996**, *35*, 1059.
- (3) (a) Rekharsky, M. V.; Inoue, Y. *Chem. Rev.* **1998**, *98*, 1875. (b) Rekharsky, M.; Inoue, Y. *J. Am. Chem. Soc.* **2000**, *122*, 4418. (c) Rekharsky, M. V.; Inoue, Y. *J. Am. Chem. Soc.* **2002**, *124*, 813.
- (4) (a) Liu, Y.; Chen, G.-S.; Chen, Y.; Ding, F.; Chen, J. *Org. Biomol. Chem.* **2005**, *3*, 2519. (b) Liu, Y.; Yang, E.-C.; Yang, Y.-W.; Zhang, H.-Y.; Fan, Z.; Ding, F.; Cao, R. *J. Org. Chem.* **2004**, *69*, 173. (c) Liu, Y.; Zhao, Y.-L.; Zhang, H.-Y.; Fan, Z.; Wen, G.-D.; Ding, F. *J. Phys. Chem. B* **2004**, *108*, 8836.
- (5) (a) Schneider, H.-J.; Hackett, F.; Rüdiger, V.; Ikeda, H. *Chem. Rev.* **1998**, *98*, 1755. (b) Szejtli, J.; Osa, T. Cyclodextrins. In *Comprehensive Supramolecular Chemistry*; Lehn, J.-M., Atwood, J. L., Davies, J. E. D., MacNicol, D. D., Vögtle, F., Eds.; Pergamon Press: New York, 1996; Vol. 3. (c) Lipkowitz, K. B.; Coner, R.; Peterson, M. A.; Morreale, A.; Shackelford, J. *J. Org. Chem.* **1998**, *63*, 732. (d) Franchi, P.; Lucarini, M.; Mezzina, E.; Pedulli, G. F. *J. Am. Chem. Soc.* **2004**, *126*, 4343. (e) Riela, S.; D'Anna, F.; Lo Meo, P.; Gruttadauria, M.; Giacalone, R.; Noto, R. *Tetrahedron* **2006**, *62*, 4323. (f) Danel, C.; Azaroual, N.; Foulon, C.; Goossens, J.-F.; Vermeersch, G.; Bonte, J.-P.; Vaccher, C. *Tetrahedron: Asymmetry* **2006**, *17*, 975.
- (6) Li, S.; Purdy, W. C. *Chem. Rev.* **1992**, *92*, 1457.
- (7) (a) Cooper, A.; MacNicol, D. D. *J. Chem. Soc., Perkin Trans. 2* **1978**, 760. (b) Fornasier, R.; Scrimin, P.; Tonellato, U. *Tetrahedron Lett.* **1983**, *24*, 5541. (c) Tabushi, I.; Kuroda, Y.; Mizutani, T. *J. Am. Chem. Soc.* **1986**, *108*, 4514. (d) Ihara, Y.; Nakanishi, E.; Nango, M.; Koga, J. *Bull. Chem. Soc. Jpn.* **1986**, *59*, 1901.
- (8) (a) Li, S.; Purdy, W. C. *Anal. Chem.* **1992**, *64*, 1405. (b) Feibush, B. F.; Woolley, C. L.; Mani, V. *Anal. Chem.* **1993**, *65*, 1130.
- (9) Kitae, T.; Takashima, H.; Kano, K. *J. Inclusion Phenom. Macrocyclic Chem.* **1999**, *33*, 345.
- (10) Rekharsky, M.; Yamamura, H.; Kawai, M.; Inoue, Y. *J. Am. Chem. Soc.* **2001**, *123*, 5360.
- (11) Yamamura, H.; Rekharsky, M.; Akasaki, A.; Araki, S.; Kawai, M.; Inoue, Y. *J. Phys. Org. Chem.* **2001**, *14*, 416.
- (12) (a) Uekama, K.; Hirayama, F.; Irie, T. *Chem. Rev.* **1998**, *98*, 2045. (b) Loftsson, T.; Järvinen, T. *Adv. Drug Delivery Rev.* **1999**, *36*, 59. (c) Liu, Y.; Chen, Y. *Acc. Chem. Res.* **2006**, *39*, 681.
- (13) Yang, C.; Nakamura, A.; Wada, T.; Inoue, Y. *Org. Lett.* **2006**, *8*, 3005.
- (14) Zhou, S.-S.; Yang, J.-O.; Baeyens, W. R. G.; Zhao, H.-C.; Yang, Y.-P. *J. Chromatogr., A* **2006**, *1130*, 296.
- (15) (a) Pereira, H. D.; Franco, G. R.; Cleasby, A.; Garratt, R. C. *J. Mol. Biol.* **2005**, *353*, 584. (b) Stoekler, J. D. Purine Nucleoside Phosphorylase: A Target for Chemotherapy. In *Developments in Cancer Chemotherapy*; Glazer, R. I., Ed.; CRC Press: Boca Raton, FL, 1984; p 35. (c) Obika, S.; Hari, Y.; Sekiguchi, M.; Imanishi, T. *Chem.-Eur. J.* **2002**, *8*, 4796.
- (16) (a) Nagatsugi, F.; Sasaki, S. *Biol. Pharm. Bull.* **2004**, *27*, 463. (b) Bailey, C.; Weeks, D. L. *Nucleic Acids Res.* **2000**, *28*, 1154.
- (17) (a) Nagai, K.; Kondo, H.; Tsuruzoe, N.; Hayakawa, K.; Kanematsu, K. *Heterocycles* **1982**, *19*, 53. (b) Nagai, K.; Hayakawa, K.; Kanematsu, K. *J. Org. Chem.* **1984**, *49*, 1022. (c) Nagai, K.; Ukai, S.; Hayakawa, K.; Kanematsu, K. *Tetrahedron Lett.* **1985**, *26*, 1735. (d) Nagai, K.; Hayakawa, K.; Ukai, S.; Kanematsu, K. *J. Org. Chem.* **1986**, *51*, 3931.
- (18) Djedaini-Pilard, F.; Perly, B.; Dupas, S.; Miocque, M.; Galons, H. *Tetrahedron Lett.* **1993**, *34*, 1145.
- (19) Liu, Y.; Liang, P.; Chen, Y.; Zhao, Y.-L.; Ding, F.; Yu, A. *J. Phys. Chem. B* **2005**, *109*, 23739.
- (20) (a) Tabanca, N.; Kirimer, N.; Demirci, B.; Demirci, F.; Baser, K. H. C. *J. Agric. Food Chem.* **2001**, *49*, 4300. (b) Cabo, J.; Crespo, M. E.; Jimenez, J.; Zarzuelo, A. *Plant. Med. Phytother.* **1986**, *203*, 213. (c) Hammerschmidt, F.-J.; Clark, A. M.; Soliman, F. M.; El-Kashoury, E.-S. A.; Abd El-Kawy, M. M.; El-Fishawy, A. M. *Planta Med.* **1993**, *59*, 68. (d) Buchbauer, G.; Jager, W.; Jirovetz, L.; Meyer, F.; Dietrich, F. *Pharmazie* **1992**, *47*, 620. (e) Başer, K. H. C.; Demirci, B.; Tabanca, N.; Özek, T. *Flavour Fragrance J.* **2001**, *16*, 195.
- (21) (a) Dodziuk, H.; Ejchart, A.; Lukin, O.; Vysotsky, M. O. *J. Org. Chem.* **1999**, *64*, 1503. (b) Schmidtchen, F. P. *Chem.-Eur. J.* **2002**, *8*, 3522. (c) Dodziuk, H.; Nowinski, K. S.; Kozminski, W.; Dolgonos, G. *Org. Biomol. Chem.* **2003**, *3*, 581. (d) Anczewski, W.; Dodziuk, H.; Ejchart, A. *Chirality* **2003**, *15*, 654.
- (22) (a) Liu, Y.; Han, B.-H.; Sun, S.-X.; Wada, T.; Inoue, Y. *J. Org. Chem.* **1999**, *64*, 1487. (b) Liu, Y.; You, C.-C.; Wada, T.; Inoue, Y. *J. Org. Chem.* **1999**, *64*, 3630.
- (23) Petter, R. C.; Salek, J. S.; Sikorski, C. T.; Kumaravel, G.; Lin, F.-T. *J. Am. Chem. Soc.* **1990**, *112*, 3860.
- (24) Rekharsky, M. V.; Schwarz, F. P.; Tewari, Y. B.; Goldberg, R. N.; Tanaka, M.; Yamashoji, Y. *J. Phys. Chem.* **1994**, *98*, 4098.
- (25) Danil de Namor, A. F.; Traboulsi, R.; Levis, D. F. V. *J. Chem. Soc., Chem. Commun.* **1990**, 751.
- (26) (a) Kajtár, M.; Horvath-Toro, C.; Kuthi, E.; Szejtli, J. *Acta Chim. Acad. Sci. Hung.* **1982**, *110*, 327. (b) Kodaka, M. *J. Am. Chem. Soc.* **1993**, *115*, 3702.
- (27) (a) Ueno, A. *Supramol. Sci.* **1996**, *3*, 31. (b) Ueno, A.; Ikeda, A.; Ikeda, H.; Ikeda, T.; Toda, F. *J. Org. Chem.* **1999**, *64*, 382. (c) Ikeda, H.; Nakamura, M.; Ise, N.; Oguma, N.; Nakamura, A.; Ikeda, T.; Toda, F.; Ueno, A. *J. Am. Chem. Soc.* **1996**, *118*, 10980.
- (28) Liu, Y.; You, C.-C.; Wada, T.; Inoue, Y. *Supramol. Chem.* **2000**, *12*, 299.
- (29) Liu, Y.; Li, L.; Zhang, H.-Y. Induced Fit. In *Encyclopedia of Supramolecular Chemistry*; Atwood, J. L., Steed, J. W., Eds.; Marcel Dekker: New York, 2004; Ch. 1.
- (30) Douteau-Guével, N.; Coleman, A. W.; Morel, J.-P.; Morel-Desrosiers, N. *J. Chem. Soc., Perkin Trans. 2* **1999**, 629.